Land use change analysis using spectral similarity and vegetation indices and its effect on runoff and sediment yield in tropical environment

N Christanto[1], J Sartohadi[1], M A Setiawan[1], D B P Shrestha[2,] and V G Jetten[2]

[1]Department of Environmental Geography, Faculty of Geography, Universitas Gadjah Mada, Indonesia
[2]Faculty of Geo-Information Science and Earth Observation (ITC), Twente University, The Netherlands

n.christanto@gmail.com

Abstract. Land use change influences the hydrological as well as landscape processes such as runoff and sediment yields. The main objectives of this study are to assess the land use change and its impact on the runoff and sediment yield of the upper Serayu Catchment. Land use changes of 1991 to 2014 have been analyzed. Spectral similarity and vegetation indices were used to classify the old image. Therefore, the present and the past images are comparable. The influence of the past and present land use on runoff and sediment yield has been compared with field measurement. The effect of land use changes shows the increased surface runoff which is the result of change in the curve number (CN) values. The study shows that it is possible to classify previously obtained image based on spectral characteristics and indices of major land cover types derived from recently obtained image. This avoids the necessity of having training samples which will be difficult to obtain. On the other hand, it also demonstrates that it is possible to link land cover changes with land degradation processes and finally to sedimentation in the reservoir. The only condition is the requirement for having the comparable dataset which should not be difficult to generate. Any variation inherent in the data which are other than surface reflectance has to be corrected.

1. Introduction

Land degradation is a common problem threatening food security and deterioration of the environment [8][9]. In the degradation processes bio-physical factors play an important role while land cover/land use changes often work in triggering or accelerating the process[7][10]. The main cause of land cover change which occurred in various parts of the world is often due to increase of population which forces the clearing of natural forest in order to create land for cultivation[15][17][26][29][36]. Other causes for deforestation leading to land cover changes are shifting cultivation [1][20][23], commercial farming (rubber, cotton, plantation of fast growing trees for fuel wood), governmental policy change[6][13][30] or due to conflicts or political cause [28].

When land cover/land use changes take place on marginal lands it can have detrimental effects on the land [14][16][19][39]. In order to study the impact of land use changes on land degradation it is imperative to study change pattern for which remote sensing techniques have played an important role. A variety of techniques starting from comparison of visual interpretation or classification of images obtained in different dates[5][25] to complex change detection techniques such as cross-correlogram

spectral matching, change vector analysis, object oriented technique, neural network or principal component analysis have been applied by various researchers[4][18][22][24][31][32][33][38].

In order to analyze the negative impact of land use changes it is important to know which land cover type has undergone which changes. Finding this answer is often not straight forward. Various change detection techniques are available[38] but information on only changed or unchanged-pixels or classes is not sufficient if we want to analyze the effect of land cover or land use changes on land degradation. On the other hand, if we want to assess which land cover has underdone which changes and if we have only remote sensing data from the past, generating land cover information in the absence of trainings samples will not be so straight forward. In the present paper a technique is described to derive land cover information from previously obtained remote sensing data based on spectral characteristics of recently obtained image.

2. The Methods

The main objectives of this study are to assess the land use change and its impact on the runoff and sediment yield of the upper Serayu Catchment. In this paper we describe a method to derive land cover/land use information from a watershed in central Java for the year 1991 based on the analysis of recent data (Landsat data from 1989 to 2015) and field work. The result of the land use change analysis will be compared with data of sediment measurement to see the relation between land use change ad sediment transports.

2.1. Study Area

The study area is located in the upper Serayu basin, Central Java, Indonesia (Figure 1) covering a surface area of about 95,174 Ha. The east to west axis is about 43 km and north to south corner about 29 km. The elevation varies from 225 m above sea level in the western part to more than 2000 m in the north eastern part, the highest mountain being Sumbing with an elevation of 3325 m. The area is volcanic with several active craters (Sindoro and Sumbing volcano). [37] described the geomorphology of the area as strongly eroded volcanic terrain. Geomorphologically the area is characterized by having volcanic cones, plateau (Dieng Plateau), strongly dissected mountain slopes and alluvial lowlands consisting of terraces and flood plain. The area is drained by several rivers (Merawu, Tulis, Begaluh) which join the main drainage system, the Serayu river which feeds into a reservoir which is located in the south-west lowland. The climate is equatorial tropical with mean annual rainfall varying from 1700 mm up to 4200 mm per year and mean annual temperature varying from 14 to 27^0 C.

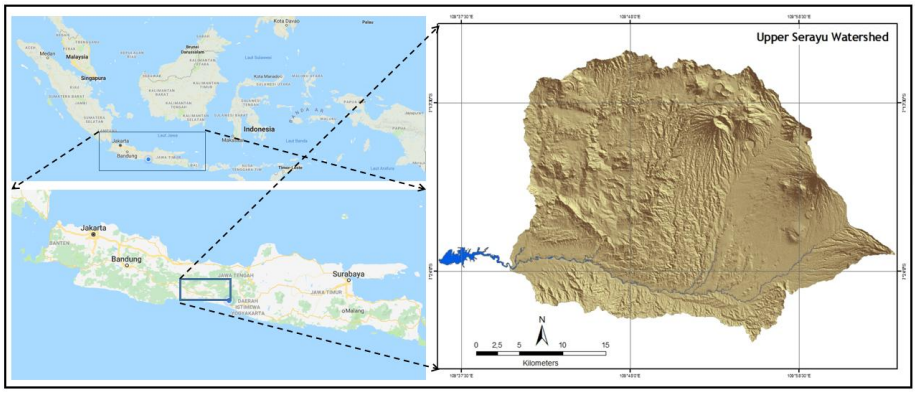

Figure 1. The study area in Serayu Watershed, Central Java, Indonesia.

2.2. Materials used and data collection

Two sets of Landsat ETM data (data acquisition 2014 and 1991) were acquired from the Serayu basin, Central Java, Indonesia. The data was geo-referenced and assigned UTM coordinates. Field work was carried out during 2014. Field observations were made using stratified random method: the first stratification is based on major land cover/land use classes. The main land cover classes identified were forest, plantation forest, dry land cultivation, paddy fields, bare soil, water body and settlements. For each land cover/land use class a number of samples points were taken which were randomly distributed, their locations were recorded using a GARMIN GPS receiver. The sample points were separated in 2 groups: one for training samples and one for validating the classification results. In addition, other data related to land degradation were also collected.

2.3. Making data comparable

In order to do land cover change analysis using remotely sensed data from different dates, it is essential to make the different datasets comparable. A data set obtained in one date has to match the radiometric and geometric parameters of other data set. Other option is to bring both the data set to a common base. Directly obtained remotely sensed image is known to have not only surface reflectance data but also artifacts caused by various factors which might be inherent in the data e.g. variations due to scattering of light, solar zenith angle, seasonal effect or due to topographic variation. Even if the two dataset are obtained in the same month there could be some difference in solar azimuth due to different acquisition dates and this could have some influence in the data.

Thus the data had to be corrected for atmospheric haze and the sensor induced gain effect which was then converted to at-sensor radiance. Finally, the at sensor radiance data were converted into top of atmosphere reflectance taking into account the solar zenith and azimuth angles based on the data acquisition date and the time. Converting the at sensor radiance value into top of atmosphere reflectance was carried out using equation and calibration data as explained in [3]. In the resulting data set pixel values represent per cent reflectance and are in the range of 0 to 100 in the corresponding spectral bands which ensure that both the data sets (1991 and 2014) are comparable and ready for further analysis.

2.4. Defining reference spectra for the main land cover classes

In order to make land cover/land use map, it is important to define reference spectra for the main land cover types. Based on the sample points taken from each land cover/land use class in the fieldwork carried out during 2014 the corresponding reflectance values were collected from the corrected Landsat TM data of 2014.

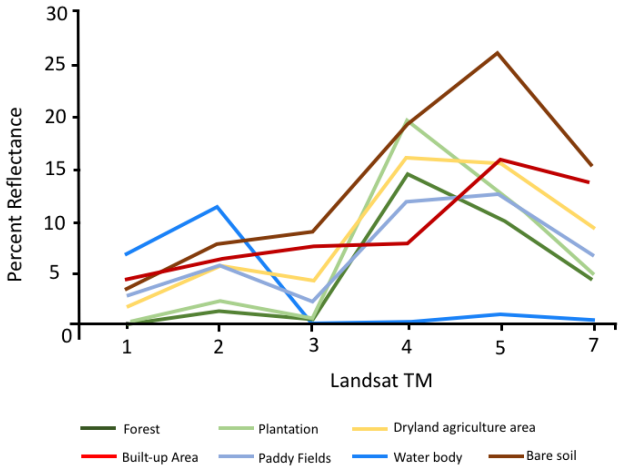

Figure 2. Spectra of various land cover/land use classes.

2.5. Generating NDVI and DVI

The reference spectral for each land cover class is derived based on the top of atmosphere reflectance data generated on Landsat of 2014. In figure 2 and in table 1 the spectra representing the main land cover/land use classes in the area are shown.

For land cover/land use classification and change detection analysis, spectral reflectance data alone may not be sufficient. The basic question on whether the land surface is covered by vegetation or not can be easily answered by using the normalized difference vegetation index (NDVI). For deriving NDVI the commonly used algorithm for Landsat Thematic Mapper bands (tm3 and tm4) is used. The resulting NDVI values are in the range of -1.0 to +1.0, the positive and higher NDVI values indicates the presence of vegetation cover while the values close to zero may mean water bodies or bare surface. For further image analysis the data with negative value is not convenient, thus it is converted into positive digital numbers (DNNDVI) as follows:

$$DN_{\mathrm{NDVI}} = 25\,NDVI + 25 \qquad (1)$$

The NDVI is multiplied by 25 and an additional 25 is added to avoid negative values which means that any pixel value of less than 25 means that it is not covered by vegetation. Thus the resulting index (DNNDVI) can be used to separate between vegetation cover from bare surfaces. But it cannot be used to differentiate between different vegetation types since it is not sensitive to variations of the difference between the reflectance in near infrared and red. For an example plantation forest and natural forest cover may show similar DNNDVI value (table 1) but the plantation forest cover has relatively higher reflectance in the near infrared band because of different tree species (AlbisiaFalcataria) as compared to that of natural forest. Moreover in the plantation forest area the fast growing tree species are often intercropped with durian (*Durio zibethinus*) or salak (*Salacca zalacca*, snake skin fruit) or other field crops thus increasing the canopy cover. In order to map these differences the difference vegetation index (DVI) would be handy. The DVI is generated simply by subtracting TM3 from TM4 as follows:

$$DVI = TM4 - TM3 \qquad (2)$$

The magnitude of the DVI could then be used to differentiate the different forest types. For an example the mean DVI value of forest is 11 and that of plantation forest is 19, showing a clear difference between them, whereas their DNNVDI values shows 50 and 48 respectively which can be considered similar (table 1). For the generation of DVI the output pixel value is assigned 0 if the value of tm3 is larger than tm4. This is done in order not to have negative values in the resulting DVI image.

2.6. Deriving classification parameters

Once the reference spectra are defined and the mean DNNDVI and the DVI are generated for each cover class (table 1), the remote sensing data obtained in earlier date can be classified. The mean values in the corresponding spectral bands in each cluster are considered as being the reference for that class. Similarly, the mean DN and DVI values are generated for each land cover/land use class.

Table 1. Reference spectra for major land cover/land use types.

	Forest	Plantation forest	Dryland cultivation	Bare soil	Built up area	Paddy field	Water body
TM1	0	0	2	3	4	3	5
TM2	1	2	6	8	6	6	9
TM3	0	1	4	9	8	2	0
TM4	11	20	16	19	8	12	0
TM5	8	13	16	26	16	12	1
TM7	3	5	10	15	14	6	0
DN_{NDVI}	50	48	40	34	25	43	0
DVI	11	19	12	10	0	10	0

For land cover classification similarity index is applied. Similarity can be defined by Euclidian distance and the spectral angle between the test pixel and the reference spectra. If the Euclidian distance is within the threshold, then it is considered similar. The similarity vector ($\vec{S}$) can be computed as follows:

$$\vec{S} = \begin{pmatrix} t_1 - c_{11} \\ t_2 - c_{12} \\ t_n - c_{1n} \end{pmatrix} = \begin{pmatrix} {}^{\delta}s_1 \\ {}^{\delta}s_2 \\ {}^{\delta}s_n \end{pmatrix} \quad (3)$$

Where t1- tn are the reflectance values in the corresponding bands of the test pixel, and c11 - c1n are the corresponding reflectance values of a reference class. ${}^{\delta}$s1..${}^{\delta}$sn represent the elements of the similarity vector $\overrightarrow{\Delta S}$. From the test pixel distances are calculated to each class center. The magnitude of the similarity vector being:

$$\left|\vec{S}\right| = \sqrt{{}^{\delta}s_1{}^{2+}\,{}^{\delta}s_2{}^{2+\cdots.}\,{}^{\delta}s_n{}^{2}} \quad (4)$$

The test pixel is classified and class label is assigned according to nearest distance if that distance is within the threshold limit for that class. Threshold values are determined using statistics of the main land cover classes. The training samples collected in the field are used to find the distribution pattern (the mean and standard deviation). The class mean and standard deviation are used to derive the spread of the class. In table 2 the statistics of various cover types are given.

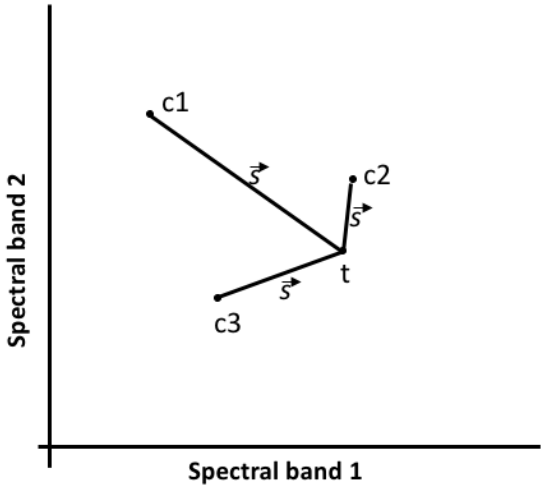

Figure 3. From the test pixel t, the similarity distances can be estimated and the one with the shortest distance to a class centre can be considered similar if it is within the threshold value from that class centre.

So, spread of reflectance value (95% confidence interval) from its mean in any spectral band for a given class can be estimated using its mean ($\bar{x}c11$) and the standard deviation ($sc11$) as follows:

$$Spread_{c11} = (\bar{x}_{c11} \pm 1.96\, s_{c11}) \quad (5)$$

The magnitude of the class spread from its center location can be estimated as:

$$|C_1| = \sqrt{((1.96\, s_{c11} - \bar{x}_{c11})^2 + (1.96\, s_{c12} - \bar{x}_{c12})^2 \ldots . (1.96\, s_{c1n} - \bar{x}_{c1n})^2} \quad (6)$$

Similarly, spectral angle is also checked if the test pixel is similar to a class. Spectral angles are computed between test pixel and the reference spectra which is given by (Kruse, Lefkoff et al. 1993) as follows:

$$Spectral\ angle = cos^{-1}\left(\frac{\sum_{i=1}^{n} t_i\, c1_i}{(\sum_{i=0}^{n} t_i)^{0.5}(\sum_{i=0}^{n} c1_i)^{0.5}}\right) \quad (7)$$

Final assignment of the class label is done by checking the corresponding DNNDVI and the DVI values if they are also within the threshold limits for that class.

2.7. Classification

It is cumbersome to compute classification on a pixel by pixel basis thus it is performed in two steps: (i) first grouping of spectrally similar classes is done by unsupervised clustering, and (ii) assigning class label to the generated cluster based on similarity measures. The iterative self-organized unsupervised clustering algorithm (ISODATA) of ERDAS Imagine software was used to do grouping of spectrally similar classes. A separate dataset was created which consists of 6 bands of Landsat TM, DNNDVI and DVI. A series of unsupervised classification runs was implemented on this new dataset with a predefined number of classes starting from 5 with an increase of one in every step and with maximum number of iterations of 50. The convergence threshold was set to 1.0. The divergence statistical measure of distance between generated cluster signatures by each run was used to select the optimal run [11].

Table 2. Statistics of the reflectance values of the major land use classes.

	Forest						Bare soil				
	min	mean	max	stdev	no		min	mean	max	stdev	no
b1	0	0	1	0.5	607	b1	1	3.6	6	0.933	176
b2	0	1.4	5	1.232	607	b2	4	7.9	12	1.222	176
b3	0	0.6	6	1.203	607	b3	3	9.1	16	2.127	176
B4	1	14.6	33	6.642	607	B4	13	19.1	24	2.371	176
b5	1	10.2	24	4.368	607	b5	19	26.1	33	2.473	176
b7	0	4.2	11	1.94	607	b7	8	15.3	23	2.556	176

	Dryland cultivation				
	min	mean	max	stdev	no
b1	0	1.7	6	1.02	434
b2	2	5.6	10	1.316	434
b3	1	4.2	11	1.88	434
B4	10	16.2	28	3.064	434
b5	11	15.6	21	1.766	434
b7	5	9.5	18	2.36	434

	Builtup area				
	min	mean	max	stdev	no
b1	1	4.3	16	1.581	260
b2	3	6.4	18	1.426	260
b3	1	7.7	28	2.494	260
B4	4	8	19	2.096	260
b5	10	15.9	37	2.926	260
b7	6	13.9	38	2.962	260

	Plantation forest						Water body				
	min	mean	max	stdev	no.		min	mean	max	stdev	no
b1	0	0.2	1	0.325	360	b1	0	6.6	18	3.039	271
b2	1	2.3	5	0.71	360	b2	0	11.4	23	3.909	271
b3	0	0.8	4	0.708	360	b3	0	0	0	0	271
B4	13	19.7	28	2.572	360	B4	0	0.3	10	1.254	271
b5	8	12.8	19	1.814	360	b5	0	0.8	8	1.033	271
b7	3	4.8	9	0.918	360	b7	0	0.3	4	0.623	271

	Paddy				
	min	mean	max	stdev	no
b1	0	2.8	9	1.033	642
b2	3	5.9	12	1.15	642
b3	0	2.3	11	1.91	642
B4	5	11.9	22	2.829	642
b5	2	12.8	27	3.96	642
b7	1	6.8	17	2.459	642

The optimal run with a distinguished peak in divergence separability explains the optimal size of spectrally similar groups [12]. In case of 1991 data, the highest divergence value of 3645 was obtained for 28 classes (figure 4). Once the optimal number of groupings is made, they can be linked to class label using the similarity parameters as explained in section 3.5. For assigning the final class label to the spectrally similar groups, the following procedure was followed.

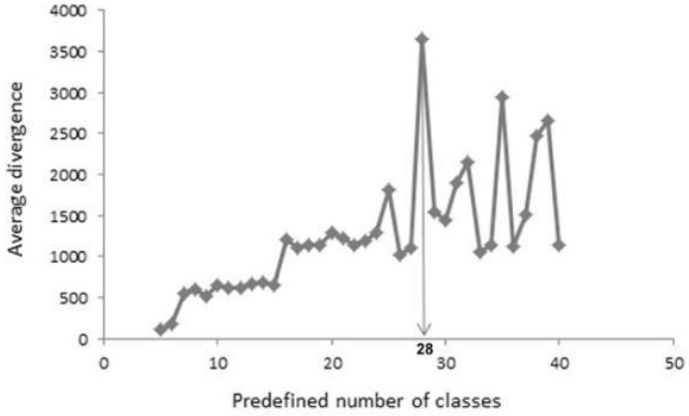

Figure 4. Average divergence values versus number of predefined number of classes in unsupervised classification.

Condition 1

- Euclidian distance and the spectral angle to a class under consideration has to be minimum of all the distances and that distance should be within the limit set by the class spread for the corresponding class (Table 3.). If there is discrepancy, then the spectral angle with the lowest value will be considered.
- In addition to this the DNNDVI and the DVI values are checked if they are within the threshold limits for that class.
- If all the above criteria are fulfilled the cluster will be class labeled or else go to condition 2.

Condition 2

- The minimum Euclidian distance and the spectral angle are larger than the threshold limit for any land cover class.
- If this is the case then the class label "Unknown" will be assigned to the cluster.

- In addition to the classification using similarity measures, the maximum likelihood classification algorithm using training samples collected during the fieldwork was also applied for 2014 image. This was done to compare the results of two classification methods.

Table 3. Euclidian distances from the resulting classes of unsupervised classification results to established land cover classes, the one with minimum distance will be class labelled.

Unsupervised Classes	Forest	Plantation forest	Dry land cultivation	Bare soil	Built up area	Paddy fields	Water body
1	15.34	8.56	**5.68**	13.82	13.96	10.18	26.69
2	18.74	16.65	8.97	11.79	**6.56**	12.02	26.08
3	13.86	**5.89**	7.78	17.26	16.87	10.47	26.19
4	14.35	**5.83**	10.99	20.39	20.26	12.69	27.12
5	19.91	13.99	**7.6**	8.73	12.15	13.53	29.98
6	19.53	**9.89**	13.88	20.25	23.5	17.27	32.23
7	20.12	11.38	**9.41**	12.48	17.71	15.16	31.91
8	18.34	**8.89**	10.84	17.05	20.23	14.94	30.75

2.8. Classification Accuracy Assessment

A set of field sample points was set aside for testing the classification accuracy for 2014 image.

3. Results and Discussions

3.1. Classification of the recent image

Result of the land cover classification for 2014 image using similarity measures is given in figure 5. The result shows that the watershed covers highest surface cover by plantation forest (54%) which is followed by primary forest (21%) and dry land cultivation (13%) (table 6). Overall accuracy of classification which is obtained by the total correctly classified pixels over total number of test pixels is 77 %t with 75 % of reliability (table 4).

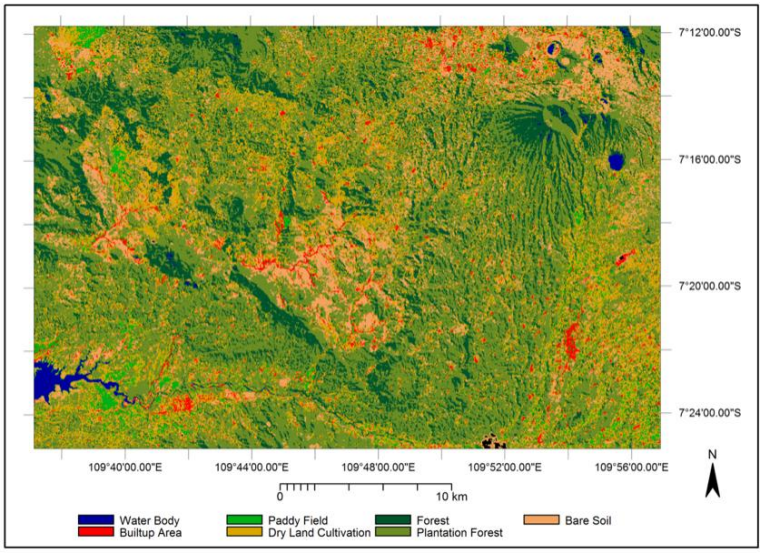

Figure 5. Land cover in 2014.

The result of applying the maximum likelihood algorithm on the same data set shows overall accuracy of 68 percent which is lower than that of applying similarity measures (table 5). Also maximum likelihood classification resulted in lot of pixels being undefined or unclassified (5 % of the total area which include also water bodies being classified as unknown). In both the classifications paddy field scored the lowest accuracy (35 %).

Table 4. Accuracy assessment of similarity measures.

	Test pixels	Water Body	Builtup Area	Paddy Field	Dry Land Cultivation	Forest	Plantation Forest	Bare Soil	Accuracy
Water body	409	391	0	0	0	18	0	0	0.96
Builtup area	135	0	115	12	0	0	0	8	0.85
Paddy	165	0	1	58	10	137	5	0	0.35
Dry land cult.	117	0	0	16	67	12	15	7	0.57
Forest	967	0	0	0	23	601	343	0	0.62
Pl. forest	882	0	0	1	9	32	840	0	0.95
Bare soil	71	0	0	0	35	0	0	36	0.51
	Reliability	1.00	0.99	0.67	0.47	0.75	0.70	0.71	

Table 5. Accuracy assessment of maximum likelihood.

	Test pixels	Water Body	Builtup Area	Paddy Field	Dry Land Cultivation	Forest	Plantation Forest	Bare Soil	Accuracy
Water body	409	393	0	0	0	1	3	0	0.96
Builtup area	135	0	75	0	0	0	0	11	0.56
Paddy	165	0	0	56	9	12	4	0	0.34
Dry land cult.	117	0	0	1	65	14	1	5	0.75
Forest	967	0	0	0	2	572	376	0	0.59
Pl. forest	882	0	0	0	14	233	635	0	0.72
Bare soil	71	0	1	0	7	0	0	63	0.89
		1.00	0.99	0.98	0.67	0.69	0.62	0.80	

3.2. Classification of 1991image

The reference spectra based on 2014 data (table 1) was applied to classify 1991 image following similarity measures as explained in section 2.6. The result shows the highest surface cover by plantation forest (45 %) and dry land cultivation (21 %) which is followed by primary forest (18 %) (figure 6).

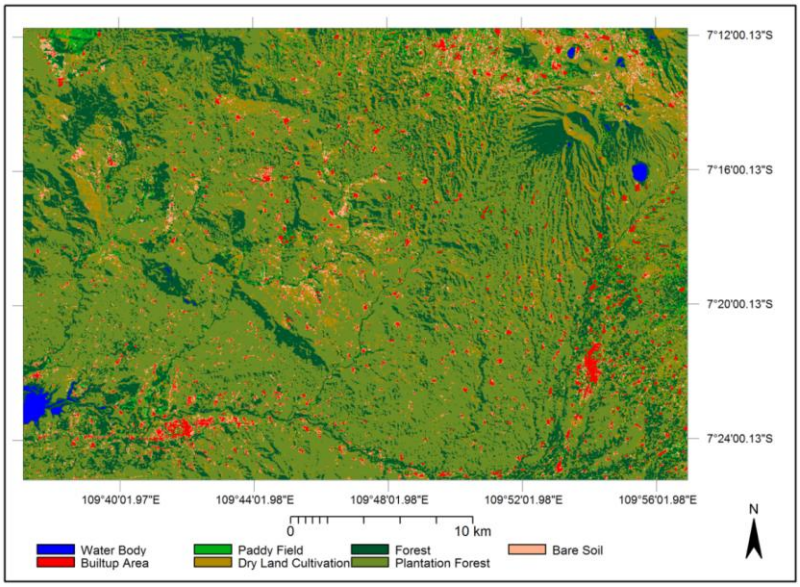

Figure 6. Lands cover classification of 1991 image.

Land cover map is not available from early nineties to validate the accuracy of the applied method but wide spread land use change in the form of deforestation to increase land for cultivation and to implement the government sponsored introduction of fast growing trees for increasing the production of the area is reported in the Serayu watershed [27]. The widespread deforestation in the early nineties in the watershed resulted in very high soil erosion in the steep slopes with the consequent deposit of high amount of suspended sediment in the Mrica reservoir, located in the southwest lowlands of the Serayu basin. The annual deposit of suspended sediment in the reservoir in 1991 (6,018,471 m^3) is considered to be the year with one of the highest recorded annual sediment deposition in the reservoir (figure 7).

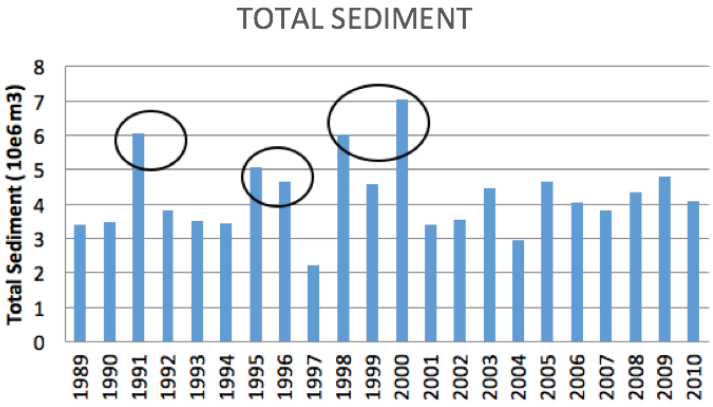

Figure 7. Suspended sediment deposition in the reservoir.

This can be used as an evident to validate the land cover classification performed in Landsat TM 1991 data. Estimation of the yearly deposit of suspended sediment is based on daily measurement of sediments at the intake of the reservoir. This data then calibrated with bathymetry measurements which also done on a yearly basis. The data is available for the year 1989 – 2010. From figure 7 we can understand that high sedimentation in 1991, 1998 and 2000 and relatively lower sediment deposition in the year 2009.

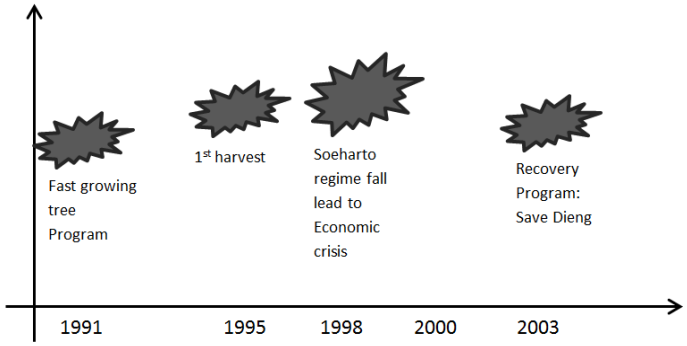

Figure 8. Major land use change policies in Indonesia.

By comparing land-use/cover in 1991 and 2014, we can see that in 1991 image there are significant bare lands in the study area. Most of the bare land is belong to Merawu catchment, and if we compare from figure 7 we can see that in 1991 the erosion rate from the Merawu Catchment is significantly high. Using this evident, we can claim that most of the erosion is come from the bare land. In the other hands, if we take a look at figure 8, we can see that in early 90's, the government has a program for a

community forest. Therefore, to meet the land needs for the community forest, some land clearing was done. This fact is another evident that the image in the 1991 is qualitatively correct.

3.3. Land covers change from 1991 to 2014

The results of the land cover classification of 1991 and 2014 shows the highest changes in plantation forest and dry land cultivation in the area. Plantation forest cover is increased in 2014 by 8391 ha (9.27 % of the whole area) and the dry land cultivation area is decreased by 7348 ha (8.11 %) (table 6). Paddy field area is increased by 1.49 %. High soil erosion in the Serayu watershed resulting in high sedimentation in the Mrica reservoir is very much related to government sponsored land use policies in the area. In early nineties community forest program (called *sengonisasi* in Indonesian) was introduced to increase the economic condition of the Serayu basin [27]. Land was cleared to implement this program. The government introduced fast growing trees called Sengon laut (*Paraserianthesfalcataria*) in the area which grows fast enough to be ready for harvest after 4-5 years thus increasing the income of the people living there.

The result of the first harvest of the fast growing trees in 1995 had led to high soil losses and high sedimentation in the reservoir (figure 5). In 1998 there was again economic crisis in Indonesia following the fall of the Soeharto regime and the global economic crisis which led to high unemployment problem (figure 6). Since the education level in Dieng plateau and its surrounding area is low [2], agriculture is the only sector that could absorb large number of labours [34]. The increase of agricultural activity in the area has led to more forest clearing which increases soil erosion significantly. This high rate of erosion not only creates a major problem in the agricultural area, but also sedimentation problem in the reservoir built for hydro power generation (figure 7).

Table 6. Land cover change from 1991 to 2014.

Land cover/land use class	1991		2014		Land cover change from 1991 to 2014
	Area (ha)	Area (%)	Area (ha)	Area (%)	Area (ha)
Water body	713	0.79	368	0.41	-345
Built up area	2403	2.65	2606	2.88	+203
Paddy field	2900	3.2	4253	4.7	+1353
Dry land cultivation	19312	21.34	11964	13.22	-7348
Forest	16169	17.86	19375	21.44	+3206
Plantation forest	40337	44.57	48728	53.84	+8391
Bare soil	8593	9.49	3214	3.55	-5379
unknown/unclassified	81	0.09	0	0	Note:
Total	90508	100.00	90508	100.00	+ increase - decrease

4. Conclusion

The main objective of this study was to assess the land use change and its impact on the runoff and sediment yield of the upper Serayu Catchment. Two period of land use analysis was done from 1991 to 2014 using Landsat imagery reveals that there is a significant land use changes. Largest increase on the area was found on plantation forest followed by forest, paddy fields and built up area. The changes were 8391 ha, 3206, 1353 and 203 respectively. Dry land cultivation and bare soil were reduce significantly during the last decade by -7348 ha and -5379 ha. The result then compared with the sediment measurement. Taking into account the results of the land use analysis, we can conclude that the sediment was decrease significantly due to land use changes.

The study shows that it is possible to classify previously obtained image based on spectral characteristics and indices of major land cover types derived from recently obtained image. This avoids the necessity of having training samples which will be difficult to obtain. On the other hand, it

also demonstrates that it is possible to link land cover changes with land degradation processes and finally to sedimentation in the reservoir. The only condition is the requirement for having the comparable dataset which should not be difficult to generate. Any variation inherent in the data which are other than surface reflectance has to be corrected.

References

[1] Angelsen A 1995 Shifting cultivation and "deforestation": A study from Indonesia. *World Development*, *23*(10), 1713–1729. http://doi.org/10.1016/0305-750X(95)00070-S.

[2] BPS 1998 Wonosobo Dalam Angka. Wonosobo, Badan Pusat Statistik.

[3] Chander G Markham B L and Helder D L 2009 Summary of current radiometric calibration coefficients for Landsat MSS, TM, ETM+, and EO-1 ALI sensors. *Remote Sensing of Environment*, *113*(5), 893–903. http://doi.org/10.1016/J.RSE.2009.01.007.

[4] Chen X Chen J Shen M and Yang W 2008 Land-use/land-cover change detection using change-vector analysis in posterior probability space. In L. Liu, X. Li, K. Liu, X. Zhang, & X. Wang (Eds.) (Vol. 7144, p. 714405). *International Society for Optics and Photonics*. http://doi.org/10.1117/12.812671.

[5] Chen Z and Wang J 2010 Land use and land cover change detection using satellite remote sensing techniques in the mountainous Three Gorges Area, China. *International Journal of Remote Sensing*, *31*(6), 1519–1542. http://doi.org/10.1080/01431160903475381.

[6] Chipika J T and Kowero G 2000 Deforestation of woodlands in communal areas of Zimbabwe: is it due to agricultural policies? *Agriculture, Ecosystems & Environment*, *79*(2–3), 175–185. http://doi.org/10.1016/S0167-8809(99)00156-5.

[7] Christanto N 2008 *Hydrological – Slope Stability Modeling for Landslide Hazard Assessment by means of GIS and Remote Sensing Data in Geo-Information for Spatial Planning and Risk Management*. Retrieved from https://www.itc.nl/library/papers_2008/msc/ugm/nugroho.pdf.

[8] Christanto N Hadmoko D S Westen C J Lavigne F Sartohadi J and Setiawan M A 2009 Characteristic and Behavior of Rainfall Induced Landslides in Java Island, Indonesia : an Overview. *EGU General Assembly 2009, Held 19-24 April, 2009 in Vienna, Austria http://meetings.copernicus.org/egu2009, p.4069*, *11*, 4069. Retrieved from http://adsabs.harvard.edu/abs/2009EGUGA..11.4069C.

[9] Christanto N Sartohadi J Setiawan M A Hadi M Jetten V G and Shrestha D P 2017 Investigating The Effect of Conservation Techniques on the Land Degradation of Tropical Catchment Prone to Landslide. *Jurnal Geografi, UNNES*, *14*(2), 1–10.

[10] Christanto N Shrestha D P Jetten V G and Setiawan M A 2012 Modeling the effect of terraces on land degradation in tropical upland agricultural area. *EGU General Assembly 2012, Held 22-27 April, 2012 in Vienna, Austria., p.1075*, *14*, 1075. Retrieved from http://adsabs.harvard.edu/abs/2012EGUGA..14.1075C.

[11] Davis S M Landgrebe D A Phillips T L Swain P H Hoffer R M Lindenlaub J C and Silva L F 1978 Remote sensing: The quantitative approach. *New York, McGraw-Hill International Book Co., 1978. 405 P.* Retrieved from http://adsabs.harvard.edu/abs/1978mhi..book.....D.

[12] de Bie C A J M Khan M R Smakhtin V U Venus V Weir M J C and Smaling E M A 2011 Analysis of multi-temporal SPOT NDVI images for small-scale land-use mapping. *International Journal of Remote Sensing*, *32*(21), 6673–6693. http://doi.org/10.1080/01431161.2010.512939.

[13] Deacon R T 1995 Assessing the Relationship between Government Policy and Deforestation. *Journal of Environmental Economics and Management*, *28*(1), 1–18. http://doi.org/10.1006/JEEM.1995.1001.

[14] Hartemink E Veldkamp T and Bao Z 2008 Property rights, land conflicts and deforestation in the Eastern Amazon. *Turk Journal Agriculture*. Retrieved from http://citeseerx.ist.psu.edu/viewdoc/download?doi=10.1.1.367.3151&rep=rep1&type=pdf.
[15] Entwisle B Rindfuss R R Walsh S J and Page P H 2008 Population growth and its spatial distribution as factors in the deforestation of Nang Rong, Thailand. *Geoforum*, *39*(2), 879–897. http://doi.org/10.1016/j.geoforum.2006.09.008.
[16] Gebresamuel G Singh B R and Dick Ø 2010 Land-use changes and their impacts on soil degradation and surface runoff of two catchments of Northern Ethiopia. *Acta Agriculturae Scandinavica, Section B - Plant Soil Science*, *60*(3), 211–226. http://doi.org/10.1080/09064710902821741.
[17] Hamandawana H Nkambwe M Chanda R and Eckardt F 2005 Population driven changes in land use in Zimbabwe's Gutu district of Masvingo province: Some lessons from recent history. *Applied Geography*, *25*(3), 248–270. http://doi.org/10.1016/J.APGEOG.2005.03.005.
[18] Jensen J R Rutchey K Koch M S and Natumalani S n.d. lnland Wetland Ghange Detection in the Everglades Water Conservation Area 2A Using a Time Series of Normalized Remotely Sensed Data. Retrieved from https://www.asprs.org/wp-content/uploads/pers/1995journal/feb/1995_feb_199-209.pdf.
[19] Kangalawe R Y M 2010 Changing land use/cover patterns and implications for sustainable environmental management in the Irangi Hills, central Tanzania. *Environment, Development and Sustainability*, *12*(4), 449–461. http://doi.org/10.1007/s10668-009-9204-5.
[20] Kingwell-Banham E and Fuller D Q 2012 Shifting cultivators in South Asia: Expansion, marginalisation and specialisation over the long term. *Quaternary International*, *249*, 84–95. http://doi.org/10.1016/J.QUAINT.2011.05.025.
[21] Kontoes C C 2008 Operational land cover change detection using change vector analysis. *International Journal of Remote Sensing*, *29*(16), 4757–4779. http://doi.org/10.1080/01431160801961367.
[22] Li X and Yeh A G O 2002 Neural-network-based cellular automata for simulating multiple land use changes using GIS. *International Journal of Geographical Information Science*, *16*(4), 323–343. http://doi.org/10.1080/13658810210137004.
[23] Liang L Shen L Yang W Yang X and Zhang Y 2009 Building on traditional shifting cultivation for rotational agroforestry: Experiences from Yunnan, China. *Forest Ecology and Management*, *257*(10), 1989–1994. http://doi.org/10.1016/J.FORECO.2008.11.032.
[24] Maldonado F D Santos J R Dos and De Carvalho V C 2002 Land use dynamics in the semi-arid region of Brazil (Quixaba, PE): Characterization by principal component analysis (PCA). *International Journal of Remote Sensing*, *23*(23), 5005–5013. http://doi.org/10.1080/0143116021000013313.
[25] Narumalani S Mishra D and Rotwell R 2004 Analyzing landscape structural change using image interpretation and spatial pattern metrics. *GIScience and Remote Sensing*.
[26] Ningal T Hartemink A E and Bregt A K 2008 Land use change and population growth in the Morobe Province of Papua New Guinea between 1975 and 2000. *Journal of Environmental Management*, *87*(1), 117–124. http://doi.org/10.1016/j.jenvman.2007.01.006.
[27] Prastowo H 1995 Pemanfaatan Produk Hutan Rakyat Sebagai Pemasok Bahan Baku Industri. Seminar Pengembangan Hutan Rakyat. D. P. d. P. S. D. Kehutanan. Bandung, Indonesia.
[28] Puppim de Oliveira J A 2008 Property rights, land conflicts and deforestation in the Eastern Amazon. *Forest Policy and Economics*, *10*(5), 303–315. http://doi.org/10.1016/J.FORPOL.2007.11.008.
[29] Rasul G Thapa G B and Zoebisch M A 2004 Determinants of land-use changes in the Chittagong Hill Tracts of Bangladesh. *Applied Geography*, *24*(3), 217–240.

http://doi.org/10.1016/J.APGEOG.2004.03.004.

[30] Redo D Millington A C and Hindery D 2011 Deforestation dynamics and policy changes in Bolivia's post-neoliberal era. *Land Use Policy*, *28*(1), 227–241. http://doi.org/10.1016/J.LANDUSEPOL.2010.06.004.

[31] Salmon B P Olivier J C Kleynhans W Wessels K J and van den Bergh F 2010 Automated land cover change detection: the quest for meaningful high temporal time series extraction. In *2010 IEEE International Geoscience and Remote Sensing Symposium* (pp. 1968–1971). IEEE. http://doi.org/10.1109/IGARSS.2010.5653723.

[32] Servello E L Kuplich T M and Shimabukuro Y E 2010 Tropical land cover change detection with polarimetric SAR data. In *2010 IEEE International Geoscience and Remote Sensing Symposium* (pp. 1477–1480). IEEE. http://doi.org/10.1109/IGARSS.2010.5653215.

[33] Su X Wu W Li H and Han Y 2011 Land-Use and Land-Cover Change Detection Based on Object-Oriented Theory. In *2011 International Symposium on Image and Data Fusion* (pp. 1–4). IEEE. http://doi.org/10.1109/ISIDF.2011.6024300.

[34] Sunderlin W D Angelsen A Resosudarmo D P Dermawan A and Rianto E 2001 Economic Crisis, Small Farmer Well-Being, and Forest Cover Change in Indonesia. *World Development*, *29*(5), 767–782. http://doi.org/10.1016/S0305-750X(01)00009-2.

[35] Svoray T and Ben-Said S 2009 Soil loss, water ponding and sediment deposition variations as a consequence of rainfall intensity and land use: a multi-criteria analysis. *Earth Surface Processes and Landforms*, *35*(2), n/a-n/a. http://doi.org/10.1002/esp.1901.

[36] Turkelboom F Poesen J and Trébuil G 2008 The multiple land degradation effects caused by land-use intensification in tropical steeplands: A catchment study from northern Thailand. *CATENA*, *75*(1), 102–116. http://doi.org/10.1016/J.CATENA.2008.04.012.

[37] Verstappen H T (Herman T & International Institute for Aerospace Survey and Earth Sciences 2000 *Outline of the geomorphology of Indonesia : a case study on tropical geomorphology of a tectogene region : with a geomorphological map 1:5,000,000*. International Institute for Aerospace Survey and Earth Sciences. Retrieved from https://catalog.hathitrust.org/Record/004250614.

[38] Wang G Xia J and Chen J 2009 Quantification of effects of climate variations and human activities on runoff by a monthly water balance model: A case study of the Chaobai River basin in northern China. *Water Resources Research*, *45*, W00A11. http://doi.org/10.1029/2007WR006768.

[39] Zucca C Canu A and Previtali F 2010 Soil degradation by land use change in an agropastoral area in Sardinia (Italy). *CATENA*, *83*(1), 46–54. http://doi.org/10.1016/J.CATENA.2010.07.003.